Visual Tracking System for the Welding of Narrow Butt Seams in Container Manufacture

Zhiguo Yan[1), 2)], De Xu[1)]

1) Key Laboratory of Complex Systems and Intelligent Science, Institute of Automation, Chinese Academy of Sciences, Beijing 100080, P. R. China (e-mail: zhgyanchn@yahoo.com).
2) Graduate University of Chinese Academy of Sciences, Beijing 100049, P. R. China(e-mail: xude@yahoo.com).

Abstract: In this paper, a vision based seam tracking system is proposed for the butt welding in the container manufacture. First, the system structure is designed. Then, the main parts of the system are discussed. The system's working principle is analyzed. And the algorithms especially the image processing algorithm and control algorithm are proposed. Finally, experiments are conducted to demonstrate the effectiveness of the designed system and the proposed method.

Keywords: butt seam, container manufacture, image processing, welding seam tracking, vision sensor, visual control

1. INTRODUCTION

As world trade continues to grow, the demand for containers is at an all-time high. In container manufacture, welding technique plays the most important role. Although the welding technology has been developed greatly in decades, manual-controlled industrial welding vehicles are the main welding tools in the container manufacturing field at present. It's a difficult and unhealthy job to control these vehicles manually. And at the same time, the welding efficiency and quality can not be guaranteed. Although many seam tracking systems have been developed, most of them can not be applied to the container production because of the narrow butt seam of container. It is of great significance to develop the seam tracking system that can be used in the butt welding of container manufacture.

The most essential issue in the seam tracking process is how to get the information of welding seam reliably. Many kinds of sensors have been used to conduct the weld joint detection, such as arc sensor (Dilthey and Stein, 1994; Kodama, *et al*, 2001), ultrasonic sensor (Mahajan and Figueroa, 1997; Shan, *et al*, 2002), and vision sensor (Rooks, 1987; Sicard, and Levine, 1989; Wang, et al, 2004; Bae, *et al*, 2002; Peng, *et al*, 1998; Zhang, *et al*, 2004). Among these sensors, vision sensor has been considered more promising than other sensors due to its no contact, high speed, and high accuracy. Laser-based vision (Yan, *et al*, 2007; Xu, *et al*, 2004) has been proved to be more robust for industrial applications. However, the narrow joint, which is about 0.5mm width, makes it not fit for container welding.

Considering the merits of the vision sensor, a vision-based seam tracking system for the narrow butt joint in container production is developed in this paper.

The torch adjusting algorithm is also very important for a seam tracking system. The welding quality depends on it directly. Traditionally, visual servoing (Hutchinson, *et al*, 1996) is classified into two groups: position-based visual servoing and image-based visual servoing. In a position-based control system, the input is computed in 3-D Cartesian space. The convergence of the system depends on the calibration of the camera and robot. On the other hand, in an image-based control system, the input is computed in 2-D image space. And there is no need to calibrate the camera and robot accurately. Considering the configuration of the proposed seam tracking system, image-based visual servoing method is adopted as the control strategy.

The rest of the paper is organized as follows: Section 2 describes the structure and principle of the seam tracking system, including the image processing algorithm and the torch adjusting algorithm. Section 3 gives the results of the experiment. Conclusion is given in Section 4.

2. STRUCTURE AND PRINCIPLE OF SEAM TRACKING SESTEM

The overall seam tracking system is composed of an industrial welding vehicle, an industrial control computer, an industrial digital CCD camera, an IEEE1394 Interface Card, an electric welding machine and some other welding related devices.

The digital CCD camera is mounted on a bracket where the torch is attached. And the optical axis of the camera is perpendicular to the planar surface of the workpiece. Before the welding, the torch is set to the adequate position manually. Then the digital camera captures image of the welding seam, and transfers it to the industrial control computer through the

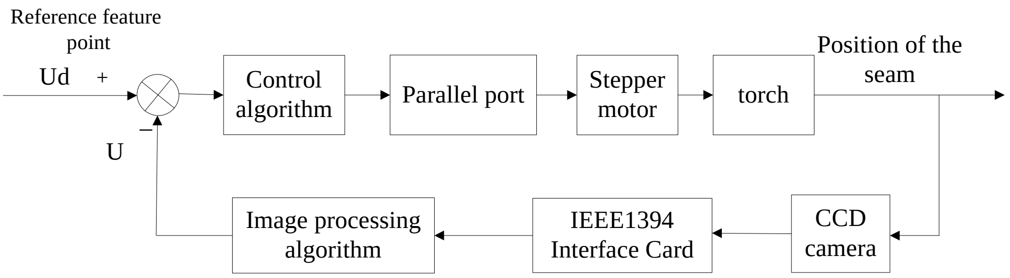

Fig. 1. Framework of the seam tracking system

IEEE1394 Interface Card. The reference feature point is determined at the beginning of the welding. To obtain a robust result, the first group of N captured images are employed to do this job. After that, the welding vehicle moves along its orbit, and the captured image is processed in real-time. The image error between the current feature point and the reference feature point can be obtained. The torch adjusting algorithm calculates the number of pulse needed to remove this image error. The industrial computer sends out control signals to the stepper motor through parallel port to align the torch along the seam according to the output of the torch adjusting algorithm. Fig.1 shows the framework of the seam tracking system.

2.1 The image processing algorithm

The image processing algorithm is the key of the proposed seam tracking system. It contains six steps: exposure time adjustment, determine the Region of Interest (ROI), get the profile of the welding seam, Hough Transform (Duda and Hart, 1972), Least-Square fitting of the straight line and calculate the feature point.

2.1.1 Exposure time adjustment

The quality of welding images is influenced greatly by the lighting. Experience indicates that images with gray level about 80 are best for processing. The processing results may be poor if the image is too dark or too bright. To avoid this kind of situations, exposure time needs to be automatically adjusted.

The criterion that is used to adjust the exposure time is the gray level of the image. The gray level is calculated as shown in equation (1). It accumulates the gray value of pixel points along the grid lines spaced ten pixels with one pixel step length.

$$S = \left(\sum_{i=1}^{W} \sum_{j=1}^{S_1} I(i,10j) + \sum_{i=1}^{S_2} \sum_{j=1}^{H} I(10i,j) \right) \Bigg/ (WS_1 + HS_2) \quad (1)$$

Where S denotes the gray level of the image; W and H are the width and height of the image; respectively. S_1=int (H/10); S_2=int (W/10); I (u, v) is the gray value of pixel point (u, v).

There is almost a linear relationship between image’s gray level and the exposure time of the camera if the aperture and the lighting are kept stable. In this paper, linear function (2) is used to approximate the relationship.

$$g = kt_e + d \quad (2)$$

Where g is the gray level, t_e is the exposure time, d and k are coefficients.

When the seam tracking system starts to work, the first two captured images are employed to adjust the exposure time. Their exposure times are set to 40ms and 50ms respectively. According to equation (1), the corresponding two gray levels are calculated and submitted to equation (2). Then coefficient k and d can be obtained easily. Let g equal to 80 and calculate out the exposure time. However, to meet the real-time requirement, the time consumed by an image capture and processing period should not be greater than 125ms.That is to say, if the acquired exposure time is greater than 125ms, set it to 125ms.

2.1.2 Determine the ROI

The image processing task will be time consuming if the seam line is detected in the whole image. To alleviate the computation burden, the ROI technology should be introduced.

In the first time of determining the ROI, the determination process is carried out in the whole image. Canny edge detector (Canny, 1986) is applied to the captured image to get its edge image E. obviously; the edge of the welding seam is sharper than the edge of other area. Notice the fact that the welding seam is about vertical in the image during the welding process. Projection of the edge information along the column direction is conducted as equation (3) illustrated.

$$P_i = \sum_{j=i-5}^{i+5} \sum_{q=1}^{S_3} E(j,5q), \quad i = 6,7,\dots W-5 \quad (3)$$

Where P_i is the projection of the i-th column, S_3 = int (H/5). E (u, v) is the value of the pixel point (u, v) of the edge image E.

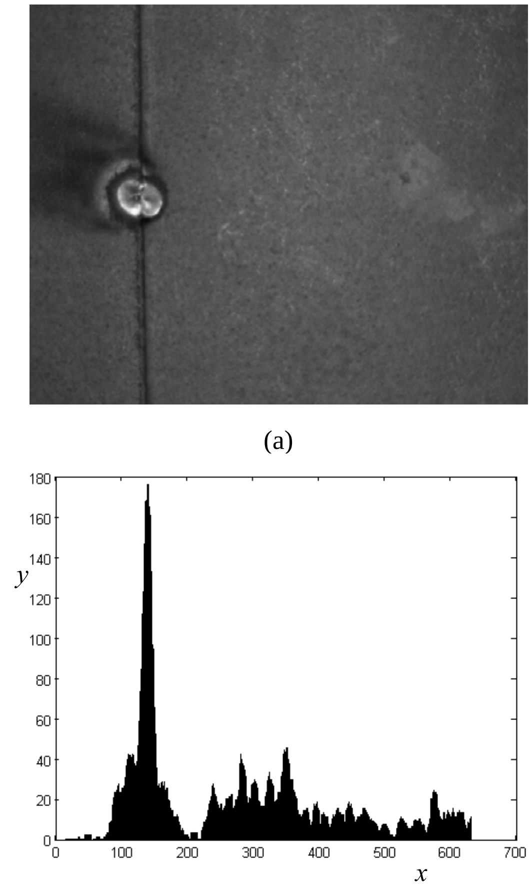

Fig. 2. A welding seam and the projection results. (a) A welding seam with a welding beading. (b) Projection results.

Fig. 2 shows a welding seam image and its projection results. Fig. 2(a) is the image of a welding seam with a welding beading on it. Fig. 2(b) shows the projection results. The x-axis is the column index of the edge image E, and y-axis is the projection results of the corresponding column. Obviously, the peak in Fig. 2(b) is the projection of the seam area, and its neighbouring region is set to be the ROI.

If the seam line in the last captured image is tracked out, the ROI can be determined easily according to the parameters of the seam line because of the continuity of time and space of the seam line in the neighbouring images.

2.1.3 Get the profile of the welding seam

The profile of the welding seam should be obtained before Hough Transform. By exploiting the fact that the gray distribution of the welding seam and the background in captured image is different along the row direction, pixel points of the seam's profile can be acquired by searching the image row by row. Fig. 3 demonstrates the gray distribution of the image in a row. The x-axis is the u-coordinate of pixel point in ROI and the y-axis means the gray value of the corresponding pixel point. Conclusion can be made easily that the lowest valley in Fig. 3 is the intersection point of the welding seam and the image row.

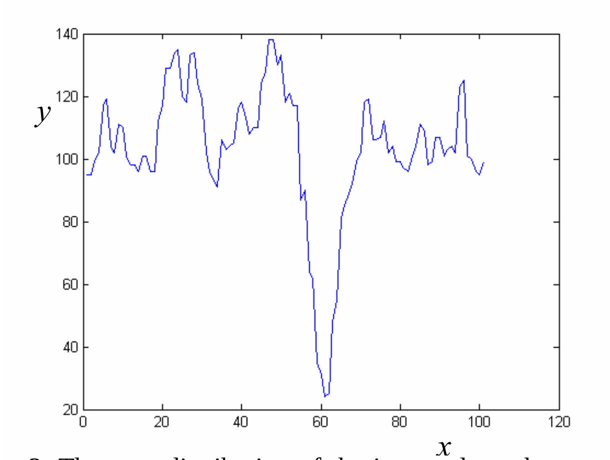

Fig. 3. The gray distribution of the image along the row direction

2.1.4 Hough Transform

Hough Transform is a widely used algorithm to detect straight lines in images. It is applied to the pixel points in the profile of the welding seam obtained in the last step to get the seam line. Here, the resolution of parameter θ in R-θ plane is set to 1 degree to accelerate the algorithm, and the range of θ is limited between 0-10 and 170-180 degrees by employing the fact that the seam line is approximately parallel to v-axis of the image. Efficiency is improved in this way.

Not all the straight lines detected are accepted as the welding seam. Under some situations, false lines may be tracked out. Considering the fact that parameter θ of the seam line is almost unchanged and parameter R varies slowly in the neighboring images during the welding process, the detected lines are eliminated if they do not satisfy the inequation (4).

$$\begin{cases} \left|R_i - \overline{R}\right| \le \Delta l \\ \left|\theta_i - \overline{\theta}\right| \le \Delta\theta \end{cases} \tag{4}$$

Where R_i, θ_i are the parameters of the straight line in i-th captured image; Δl is the distance threshold and $\Delta\theta$ is the angle threshold; $\overline{R}$ and $\overline{\theta}$ are weighted average of seam line parameters of previous p frames of images.

It should be noted that if the current seam line is removed, the ROI of the next image should be determined by projection along column direction as shown in equation (3). If the straight line satisfies inequation (4) and is kept as the welding seam, it should be transformed from the R-θ plane to the U-V plane. The line equation in the U-V plane is given as in formula (5).

$$au + bv + c = 0 \quad (5)$$

Where a, b and c are the line parameters.

2.1.5 Least-Square fitting of a Straight Line

The seam line obtained by Hough Transform is a rough one because the resolution of θ is not high enough. To get the accurate seam line, Least-squares linear fit technique is used in this step. If the distance from a pixel point in the seam profile to the line obtained by Hough Transform is less than a preset threshold l_{th}, that is to say, if a pixel point satisfies equation (6), it is accepted as the candidate pixel point.

$$(au_i + bv_i + c)\Big/\sqrt{\exp(a) + \exp(b)} < l_{th} \quad (6)$$

Least-squares linear fit technique is applied to these candidate pixel points. Equation (7), (8), (9), and (10) show the line detection process.

$$\begin{cases} \bar{u} = \sum_{i=1}^{f} u_i \\ \bar{v} = \sum_{i=1}^{f} v_i \end{cases} \quad (7)$$

$$\begin{cases} u2 = \sum_{i=1}^{f} \exp(u_i - \bar{u}) \\ uv = \sum_{i=1}^{f} (v_i - \bar{v}) * (u_i - \bar{u}) \end{cases} \quad (8)$$

Where (u_i, v_i) is the image coordinate of the i-th candidate pixel point; $(\bar{u}, \bar{v})$ is the average image coordinate of the candidate pixel points; f is the number of candidate pixel point; $u2$, uv are intermediate variables. If $u2$ is greater than zero, the straight seam line will be calculated as shown below.

$$\begin{cases} m = uv/u2 \\ n = \bar{v} - m * \bar{u} \end{cases} \quad (9)$$

Where m and n are slope and intercept of the straight seam line, respectively. If $u2$ is equal to zero, the function of the straight seam line will be in the form of equation (10).

$$u = \bar{u} \quad (10)$$

2.1.6 Calculate the feature point

The selection of the feature point is very important. Feature point is the result of the image processing algorithm and the basis of the torch adjusting algorithm. The size of image captured in this system is 640×512 in pixel, the intersection point of the welding seam and the line v=256 is selected as the feature point. Fig. 4 shows the selection of the feature points.

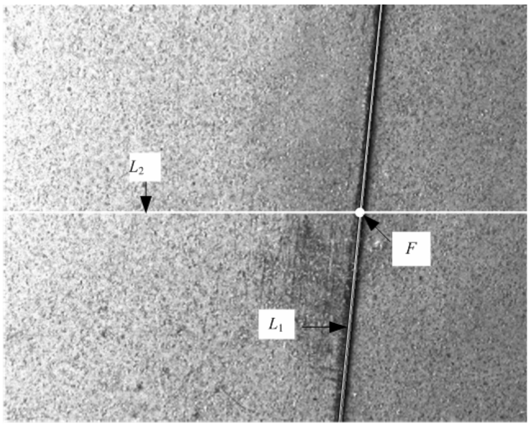

Fig. 4. The selection of the feature point

In the figure, straight line L_1 is the detected welding seam, whose expression is shown as equation (5). L_2 is the straight line v=256. Point F, the intersection point of line L_1 and L_2, whose image coordinate is $((-256b - c)/a$, 256), is selected as the feature point.

2.2 The control algorithm

During the working process of the proposed system, the area to be welded in the plate is almost planar, and it is nearly parallel to the image plane. Conclusion can be made that it is not necessary to adjust the welding torch in normal direction of the plane. Image-based visual servoing method, which is known to be robust not only with respect to camera but also to robot calibration errors, is adopted as the control strategy of the system.

According to the image processing result, the torch is adjusted in the left-right direction by the control algorithm. Before welding, the torch is set to the adequate position manually. The reference feature point (u_r, v_r) is determined according to the first group of N calculated feature points. Then, the calculated feature points and the reference feature point are used to get the image errors. The calibration result shows that the stepper motor needs about 118 pulses to remove an image error of one pixel. A PI controller is designed to determine the numbers of pulses for the stepper motors. Equation (11) shows the controller.

$$U_{pi}(r) = K_p e(r) + K_i \sum_{i=0}^{r} e(i)\Delta t \qquad r = 0, 1, 2, ... \quad (11)$$

Where $U_{pi}(r)$ and $e(r)$ are the output and the image error during the r-th sampling interval Δt; and K_p, K_i are the proportional, integral gains.

3. EXPERIMENTS AND RESULTS

To evaluate the vision-based seam tracking system, a butt welding seam, which was about 0.5mm width and 600mm length, was employed in the experiments.

The Cartesian space resolution of a pixel in image space in experimental system was 0.091mm/pixel. The velocity of the welding vehicle was about 1100mm/minute. The welding seam tracking experiments were conducted with the designed visual tracking system and the proposed methods. The image coordinate of the refer feature point was (354, 256). Fig. 5 shows the experimental results. Fig. 5(a) displays the experimental system. Fig. 5(b) gives a frame image of the captured welding seam. Fig. 5(c) shows the deviation from the torch to the welding seam when the torch was not adjusted. The *x*-axis is the moved distance of the torch from the origin along the welding seam, and the corresponding *y*-coordinate is the deviation from the torch to the welding seam. Fig. 5(d) gives the deviation from the torch to the welding seam during the seam tracking process.

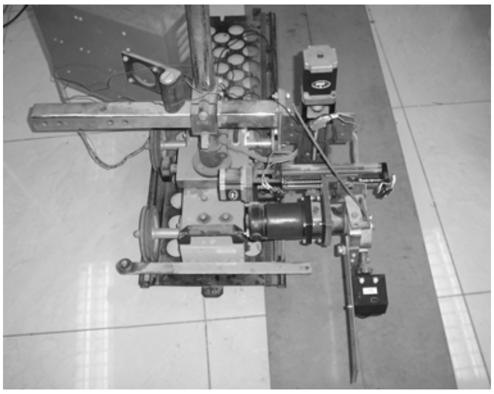

(a)

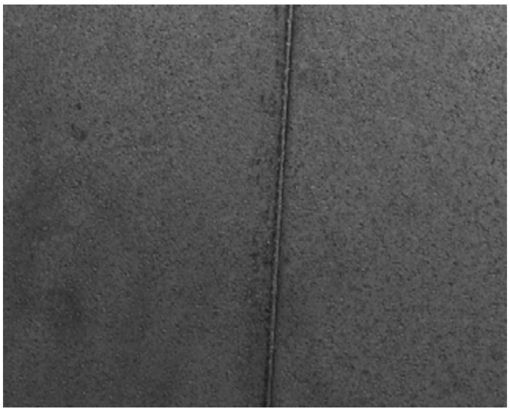

(b)

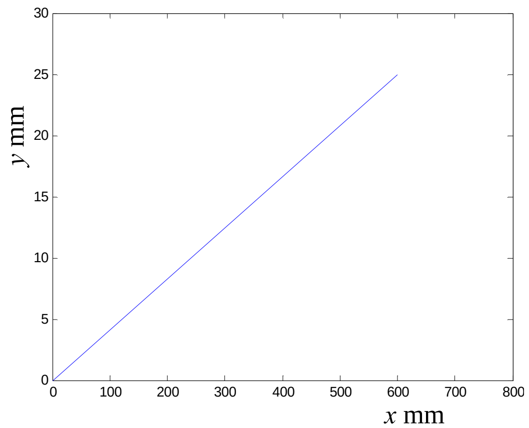

(c)

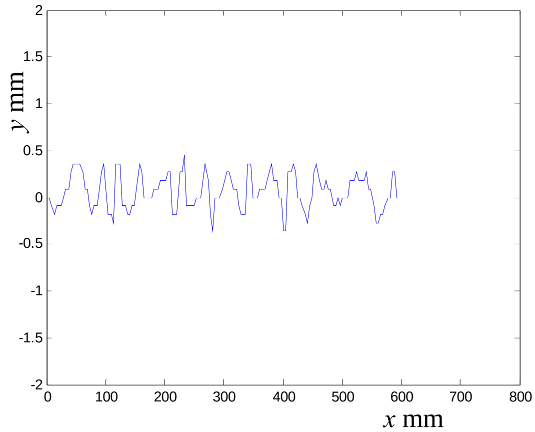

(d)

Fig. 5. Experimental results. (a) The experimental system. (b) The captured welding seam image. (c) The deviation from the torch to the seam if the torch is not adjusted. (d) The deviation from the torch to the seam during the seam tracking process.

The experimental system was tested in workshop. A 2000mm length welding seam was welded. Fig. 6 shows the welding results. The experimental results indicate that the seam tracking system can meet the requirement of container welding.

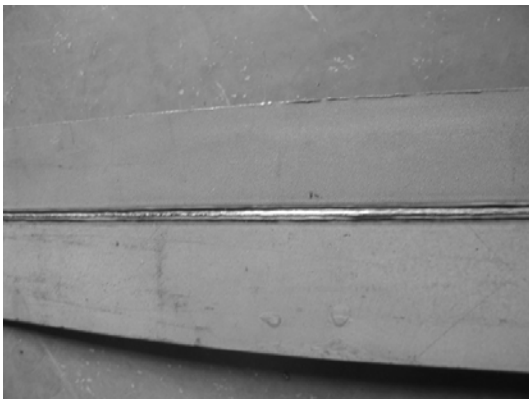

Fig. 6 The welding results

4. CONCLUSIONS

The vision-based seam tracking system proposed in this paper can improve the welding efficiency and quality of container manufacture. The torch is adjusted to track the welding seam according to the image errors acquired by image processing algorithm. The experiments give evidence that the precision of the system can meet the need of quality requirements of welding.

ACKNOWLEDGEMENT

This work is supported by the National High Technology Research and Development Program of China under grant 2006AA04Z213.

REFERENCE

Dilthey, U., Stein, L. (1994). Through the arc sensing: A multipurpose low-cost sensor for arc welding automation. *Welding in the World*, **34**, 165-171.

Kodama, M., Iwabuti, H., and Iwabuti, H. (2001). Arc sensor for simultaneous detection of torch aiming deviation and gap width-development of high frequency oscillation arc. *Welding International*, **15**(**12**), 952-964.

Mahajan, A., Figueroa, F. (1997). Intelligent seam tracking using ultrasonic sensors for robotic welding. *Robotica*, **15**(**3**), 275-281.

Shan, P., Sun, D., Tu, W. H., and Hu, S. S. (2002). Development of Seam Tracking Technology with Ultrasonic Sensor in CO2 Welding. *Transactions of the China Welding Institution,* **23**(**5**), 19-22.

Rooks, B. (1987). Vision seam tracking extends to TIG. *Industrial Robot*, **14**(**4**), 207-208.

Sicard, P., Levine, M. D. (1989). Joint recognition and tracking for robotic arc welding. *IEEE Transactions on Systems, Man and Cybernetics*, **19**(**4**), 714-728.

Wang, L. K., Xu, D., Tan, M. (2004). Robust detection for the weld seam shaped zigzag line. *In Proceedings of 2004 IEEE International Conference on Robotics and Biomimetics*, 721-726.

Bae, K. Y., Lee, T. H., and Ahn, K. C. (2002). An optical sensing system for seam tracking and weld pool control in gas metal arc welding of steel pipe, *Journal of Materials Processing Technology*, **120**(**2**), 458-465.

Peng, J., Chen, Q., Lu, J., Jin, J., and Van Luttervelt, C. A.(1998). "Real Time Optimizations of Robotic Arc Welding Based on Machine Vision and Neural Networks," *Proceedings of the 24th Annual Conference of the IEEE Industrial Electronics Society,* **3**, 1279-1280.

Zhang, H., Ding, X. L., *et al*. (2004). The seam tracking system for submerged arc welding. *Lecture Notes in Control and Information Sciences*, **299**, 144-151.

Yan, Z. G., Xu, D., Li, Y., and Tan, M. (2007). A Vision-based Seam Tracking System for Submerged Arc Welding. *RWIA 2006, Lecture Notes in Control and Information Science,* **362**, 349-357.

Xu, D., Wang, L. K., Tan, M. (2004). Image Processing and visual control method for arc welding robot. *In Proceedings of 2004 IEEE International Conference on Robotics and Biomimetics*, 727 – 732.

Duda, R. O. and Hart, P. E. (1972). Use of Hough transform to detect lines and curves in pictures, *Communication of the ACM, Association for Computing Machinery*, **15**(**1**), 11-15.

Hutchinson, S., Hager, G., Corke, P. I. (1996). A tutorial on visual servo control. *IEEE Transaction on Robotics and Automation*, **12**(**10**), 651-670.

Canny, J. (1986). A computational approach to edge detection. *IEEE Transactions on Pattern Analysis and Machine Intelligence,* **8**(**6**), 679-697.